

Novel aspects of elastic flapping wing: Analytical solution for inertial forcing

Hadi Zare^a, Seid H. Pourtakdoust^{*1} and Ariyan Bighashdel^b

Center of Excellence in Aerospace Systems, Department of Aerospace Engineering,
Sharif University of Technology, Azadi Street, Tehran, Iran

(Received June 14, 2017, Revised September 13, 2017, Accepted October 9, 2017)

Abstract. The structural dynamics (SD) behavior of Elastic Flapping Wings (EFWs) is investigated analytically as a novel approach in EFWs analysis. In this regard an analytical SD solution of EFW undergoing a prescribed rigid body motion is initially derived, where the governing equations are expressed in modal space. The inertial forces are also analytically computed utilizing the actuator induced acceleration effects on the wing structure, while due to importance of analytical solution the linearity assumption is also considered. The formulated initial-value problem is solved analytically to study the EFW structural responses, where the effect of structure-actuator frequency ratio, structure-flapping frequency ratio as well as the structure damping ratio on the EFW pick amplitude is analyzed. A case study is also simulated in which the wing is modeled as an elastic beam with shell elements undergoing a prescribed sinusoidal motion. The corresponding EFW transient and steady response in on-off servo behavior is investigated. This study provides a conceptual understanding for the overall EFW SD behavior in the presence of inertial forces plus the servo dynamics effects. In addition to the substantial analytical results, the study paves a new mathematical way to better understanding the complex role of SD in dynamic EFWs behavior. Specifically, similar mathematical formulations can be carried out to investigate the effect of aerodynamics and/or gravity.

Keywords: flapping wing; modeling; structural dynamics; aeroelasticity; inertial forcing

1. Introduction

Flapping aerial vehicles (FAVs) have attracted worldwide interest for their possible applications in a wide range of activities, such as monitoring and surveillance. FAVs use flapping wing mechanism to fly, while simultaneously producing thrust and lift. Both bird-like and insect-like flyers utilize flexible flapping wings which have anisotropic flexibilities in chordwise and spanwise directions (Shyy *et al.* 1999). Based on their structures, flapping wings undergo moderate to large flexible deformation during flight (Wootton 1992).

The flexibility has a significant effect on the FAVs aerodynamic loading (Smith 1995, Olivier

*Corresponding author, Professor, E-mail: pourtak@sharif.edu

^aPh.D. Candidate, E-mail: h_zare@ae.sharif.ir

^bM.Sc., E-mail: bighashdel_a@ae.sharif.ir

and Dumas 2016) which has frequently been validated, experimentally (Heathcote *et al.* 2008, Mazaheri and Ebrahimi 2010, Zhao *et al.* 2010). The importance of this phenomenon has led many researches to modeling the structural dynamics (SD) behavior of Elastic Flapping Wings (EFWs).

Some researchers, have modeled EFW SD by direct time integration of full order models (FOM) (Larijani and DeLaurier 2001, Nakata and Liu 2012, Pourtakdoust and Aliabadi 2012, De Rosis *et al.* 2014) and some others, because of the expensive computational cost of previous approach, have employed the reduced order model (ROM) in which FOM are transformed into a reduced basis co-ordinate system e.g. modal coordinate transformation (Singh and Chopra 2007, Kim and Han 2008).

With respect to the existence of several loads in flapping flight including aerodynamics, gravitation, structure and inertia, some researchers have compared the effect of these forces on flexibility, implicitly or explicitly. For instance, Combes and Daniel (2003) experimentally investigated the contributions of aerodynamic and inertial elastic forces for a specific wing. They compared wing bending results for normal air versus helium and showed that contribution of fluid-dynamic forces to wing deformations is significantly reduced. This relatively huge reduction in air density produced only slight changes in the pattern of the wing deformations, suggesting that fluid-dynamic forces have minimal effect on the wing bending. However, they emphasized that this claim is reliable for certain combinations of wing stiffness, wing motions, and fluid density (Daniel and Combes 2002). This conclusion proposes that in some conditions, the inertial forces effect on EFW behavior is of premier importance. In this regard, some researchers focused on inertial forces. Barut, Das *et al.* (2006) utilized finite element model (FEM) concepts in conjunction with nonlinear theory of elasticity and rigid-body dynamics to investigate the effect of prescribed dynamic motion and flexibility on the EFW deformation in absence of aerodynamic loads. Their study included the effect of inertial forces due to centrifugal and Coriolis accelerations caused by wing flapping and pitching motions as well as the stress-induced forces due to considerable stretching and bending deformations occurring in the wing. Wilson and Wereley (2007) experimentally investigated the performance of an insect-like EFW and quantified the lifting force in hover condition. They used an experimental test-stand to flap the wings with one and two degrees of freedom and measured the wing loadings. Additionally, to identify the non-aerodynamic forces, they performed their tests in a vacuum chamber as well. Yeo *et al.* (2013) also used a vacuum chamber to measure non-aerodynamic forces of an EFW.

The current study is focused on derivation of an analytical solution for Structural Dynamic Equation (SDE) of EFW that has not yet been attempted in the literature. Due to importance of inertial forces (Combes and Daniel 2003) for bird like structures, only the inertial forces are considered. Further, the effect of servo dynamics for resonance behavior is also considered. For this purpose, the SDE governing an EFW is expressed in modal space that is widely used for elasticity analysis of various flying vehicles including EFWs (Isogai and Harino 2007, Kim and Han 2008), missiles (Platus 1992, Pourtakdoust and Assadian 2004), aircrafts (Meirovitch and Tuzcu 2003) and airships (Li *et al.* 2009). In all latter studies, deflections are expanded in terms of the normal structural modes where the final governing equations are derived using the orthogonality conditions. In this scheme, the EFW natural frequencies and mode shapes are obtained via Finite Element Method (FEM). To develop an analytical solution, it is assumed that the structure responses lie within the linear range. This is valid for a low flapping frequency range that in turn yields a low flapping to structure frequency ratio. Considering this assumption, the coupling effects between various structural modes can be ignored and the governing SD equations become linear and uncoupled. The resulting analytical solution enables one to assess and evaluate

the coupling between the imposed forcing, structure and the servo dynamics, thus providing a conceptual understanding for the overall EFW SD behavior in the presence of inertial forces plus the servo dynamics effects. The remainder of this paper is organized as follows. Section 2 describes the formulation of the SDE, inertial forces and servo motor dynamics. Sections 3 and 4 are devoted to the development of the analytical solution of rigid and elastic wing motion. Section 5 delivers the verification and simulation results for a typical EFW under a various loading scenarios, followed by conclusions in Section 6.

2. Formulation

2.1 Structure model

Accurate prediction of large amplitude structural deformations is feasible via nonlinear finite element models. However, representation of complex system equations of motion in finite element nodal space requires large degrees of freedom and computational cost that is impractical for design applications (Hollkamp and Gordon 2008). The governing structural equations of motion for a multiple degree-of-freedom (DOF), geometrically nonlinear system with viscous damping can be written as (Rizzi and Muravyov 2002)

$$\mathbf{M}\ddot{\mathbf{W}}(t) + \mathbf{C}\dot{\mathbf{W}}(t) + \mathbf{K}\mathbf{W}(t) + \Psi(\mathbf{W}(t)) = \mathbf{F}(t) \tag{1}$$

where \mathbf{M} , \mathbf{C} and \mathbf{K} are the mass, damping, and stiffness matrices respectively, \mathbf{W} is the displacement vector and \mathbf{F} represents the force excitation vector. The nonlinear forcing term $\Psi(\mathbf{W}(t))$ is a nonlinear vector function of \mathbf{W} that in absence of large structural displacement can be ignored. An alternative solution approach of the above equation is via transformation to a reduced basis modal coordinate system that dramatically reduces the number of DOFs (McEwan *et al.* 2001). The generalized coordinate transformation approach is implemented to obtain a set of coupled modal equations, with reduced DOF

$$\mathbf{W} = \Phi\boldsymbol{\eta} \tag{2}$$

where $\boldsymbol{\eta}$ and Φ are time-dependent vectors of generalized coordinates and a subset of linear eigenvectors (assumed mode shapes vectors), respectively. Using the above transformation under the assumption of the low amplitude structural displacement, resulting in an uncoupled, linear system of equations as follows

$$\ddot{\eta}_r(t) + 2\zeta_r\omega_r\dot{\eta}_r(t) + \omega_r^2\eta_r(t) = N_r(t); \quad r = 1, 2, \dots \tag{3}$$

where ω_r , ζ_r are the structural undamped natural frequencies and the damping coefficients, respectively and N_r 's are the generalized forces which defined as

$$N_r(t) = \int_D \phi_r(P)\mathbf{F}(P,t)dD(P), \quad r = 1, 2, \dots \tag{4}$$

where P is an arbitrary point within the domain D.

2.2 Inertial force modelling

Due to accelerated motion of the EFW, centrifugal and normal forces are applied to each

element. Considering the inherent in-plane tensile strength of the EFW, centrifugal forces can be neglected in comparison with the normal forces. The summation of normal inertial forces applied to an element due to angular acceleration is

$$\sum_{i,j} \mathbf{F}_{z_{ij}} = a_n dm = \left\{ (y - y_0)[- \ddot{\gamma}(t)] + (x - x_0)\ddot{\theta}(t) + \left(\sqrt{x^2 + y^2} - \sqrt{x_0^2 + y_0^2} \right) \ddot{\chi}(t) \right\} dm \quad (5)$$

where \mathbf{F}_{ij} is the applied force caused by neighbouring elements, a_n is the linear acceleration, x and y are the position of the mass element dm , x_0 and y_0 are the position of the wing junction, and $\dot{\gamma}$, $\ddot{\theta}$ and $\ddot{\chi}(t)$ are the angular accelerations of the EFW due to flapping, pitching and sweeping motions, respectively. Please note that the minus sign in Eq. (5) is due to the reference definition of the γ . Thus, according to the Newton's third law of reaction, the applied inertial force from this element to EFW will be

$$d\mathbf{F}_l = \mathbf{r} \cdot \ddot{\boldsymbol{\omega}} dm = \sum_{k=1}^3 r_k \ddot{\omega}_k dm \quad ; \quad \mathbf{r} = \begin{bmatrix} y - y_0 \\ x - x_0 \\ \sqrt{x^2 + y^2} - \sqrt{x_0^2 + y_0^2} \end{bmatrix} \quad ; \quad \boldsymbol{\omega} = \begin{bmatrix} \gamma(t) \\ -\theta(t) \\ -\chi(t) \end{bmatrix} \quad (6)$$

where the subscript k refers to each kinematics DOF (KDOF). Referring to Eq. (6), one can define generalized forces as follows

$$N_r(t) = \int_D \boldsymbol{\phi}_r d\mathbf{F}_l = \sum_{k=1}^3 \ddot{\omega}_k \int_A \boldsymbol{\phi}_r r_k dm = \sum_{k=1}^3 \ddot{\omega}_k \Gamma_k \quad (7)$$

where

$$\Gamma_k = \int_A \boldsymbol{\phi}_r r_k dm \quad (8)$$

It is realized that, Γ_k turns out as structural property that depends on the structure mass distribution and is motion independent. In this sense it can be referred to as ‘‘Generalized Inertial Moment’’ or GIM.

2.3 Servo motor dynamics

The objective of the servo systems is to control the position of a mechanical system in accordance with a prescribed position. To model the servo actuator effects on the dynamic response of the EFW, a second order servo dynamics is considered whose transfer function is suggested (Ogata 2010).

3. Analytical solution of rigid wing motion

In analogy with actual flying EFWs like a bird, it is possible for the flapping motion to stop in a gliding phase of flight. Accordingly, the desired flapping motion can be broken in to a sinusoidal part followed by a command to stop the flapping at a static value. As already discussed, considering a second order transfer function for the controller, will yield,

$$\frac{\omega_k}{\omega_{input_k}}(s) = \frac{\omega_{c_k}^2}{s^2 + 2\zeta_{c_k} \omega_{c_k} s + \omega_{c_k}^2} \quad (9)$$

where ω_k and ζ_{c_k} are the undamped natural frequency and the damping ratio for k^{th} kinematic DOF.

3.1 Periodic flapping command

A periodic flapping trend that includes rotational motions about all three major axes can be represented via sine series by means of amplitude $\bar{\omega}_{\max_{k,j}}$, frequency $\omega_{k,j}$ and a phase shift $\phi_{k,j}$ as

$$\bar{\omega}_{input_k}(t) = \sum_{j=1}^{\infty} \bar{\omega}_{\max_{k,j}} \sin(\omega_{k,j}t + \phi_{k,j}) \tag{10}$$

Please note that in real flapping motion all, the frequencies are equal or a product of a specific frequency (ω).

Subsequently, using Laplace transformations results in

$$\varpi_k(t) = \sum_{j=1}^{\infty} e^{-\zeta_{c_k} \omega_{c_k} t} A_{22_{k,j}} \sin(\omega_{dc_k} t + \phi_{22_{k,j}}) + A_{11_{k,j}} \sin(\omega_{k,j} t + \phi_{11_{k,j}}) \tag{11}$$

with the following parameters that are defined for sensitivity analysis of the EFW response,

$$\omega_{dc_k} = \omega_{c_k} \sqrt{1 - \zeta_{c_k}^2} \tag{12}$$

$$A_{21_{k,j}} = \frac{\bar{\omega}_{\max_{k,j}}}{1 - 2 \left(\frac{\omega_{k,j}}{\omega_{c_k}} \right)^2 (1 - 2\zeta_{c_k}^2) + \left(\frac{\omega_{k,j}}{\omega_{c_k}} \right)^4} \tag{13}$$

$$A_{22_{k,j}} = A_{21_{k,j}} \left\{ \left(2\zeta_{c_k} \frac{\omega_{k,j}}{\omega_{c_k}} \cos \phi_{k,j} + \left(\left(\frac{\omega_{k,j}}{\omega_{c_k}} \right)^2 - 1 \right) \sin \phi_{k,j} \right)^2 + \frac{1}{\sqrt{1 - \zeta_{c_k}^2}} \left(\left(2 \frac{\omega_{k,j}}{\omega_{c_k}} \zeta_{c_k}^2 - \frac{\omega_{k,j}}{\omega_{c_k}} + \left(\frac{\omega_{k,j}}{\omega_{c_k}} \right)^3 \right) \cos \phi_{k,j} + \left(\left(\frac{\omega_{k,j}}{\omega_{c_k}} \right)^2 - 3 \right) \zeta_{c_k} \sin \phi_{k,j} \right)^2 \right\}^{1/2} \tag{14}$$

$$A_{11_{k,j}} = A_{21_{k,j}} \sqrt{\left(2\zeta_{c_k} \frac{\omega_{k,j}}{\omega_{c_k}} \cos \phi_{k,j} + \left(\left(\frac{\omega_{k,j}}{\omega_{c_k}} \right)^2 - 1 \right) \sin \phi_{k,j} \right)^2 + \left(\left(1 - \left(\frac{\omega_{k,j}}{\omega_{c_k}} \right)^2 \right) \cos \phi_{k,j} + 2\zeta_{c_k} \frac{\omega_{k,j}}{\omega_{c_k}} \sin \phi_{k,j} \right)^2} \tag{15}$$

$$\phi_{11_{k,j}} = \tan^{-1} \left(\frac{2\zeta_{c_k} \frac{\omega_{k,j}}{\omega_{c_k}} \cos \phi_{k,j} + \left(\left(\frac{\omega_{k,j}}{\omega_{c_k}} \right)^2 - 1 \right) \sin \phi_{k,j}}{\left(1 - \left(\frac{\omega_{k,j}}{\omega_{c_k}} \right)^2 \right) \cos \phi_{k,j} + 2\zeta_{c_k} \frac{\omega_{k,j}}{\omega_{c_k}} \sin \phi_{k,j}} \right) \tag{16}$$

$$\phi_{22_{k,j}} = \tan^{-1} \left(\frac{\sqrt{1 - \zeta_{c_k}^2} \left(2\zeta_{c_k} \frac{\omega_{k,j}}{\omega_{c_k}} \cos \phi_{k,j} + \left(\left(\frac{\omega_{k,j}}{\omega_{c_k}} \right)^2 - 1 \right) \sin \phi_{k,j} \right)}{\left(2 \frac{\omega_{k,j}}{\omega_{c_k}} \zeta_{c_k}^2 - \frac{\omega_{k,j}}{\omega_{c_k}} + \left(\frac{\omega_{k,j}}{\omega_{c_k}} \right)^3 \right) \cos \phi_{k,j} + \left(\left(\frac{\omega_{k,j}}{\omega_{c_k}} \right)^2 - 3 \right) \zeta_{c_k} \sin \phi_{k,j}} \right) \tag{17}$$

3.2 Stopping command

In the stopping command case, it is assumed that the EFW flapping is suddenly commanded to perform a stopping manoeuvre at k^{th} KDOF towards a fixed angle at t_i , such that

$$\varpi_{\text{input}_k} = \Delta \varpi_{\text{glide}_k} ; \Delta \varpi_{\text{glide}_k} = \varpi_{\text{Stop}_k} - \varpi_k(t_i) \quad (18)$$

where $\varpi_k(t_i)$ and ϖ_{Stop_k} are the current and final angles of the EFW for a final glide operation at k^{th} KDOF, respectively. Again, via Laplace transformation, one can show the actual commanded result due to the servo dynamic to be as follows

$$\varpi_k(t) = \varpi_{\text{Stop}_k} - e^{-\zeta_{c_k} \omega_{c_k} t} B_{11_k} \sin(\omega_{dc_k} t + \psi_{11_k}) \quad (19)$$

where

$$B_{11_k} = \frac{\Delta \varpi_{\text{glide}_k}}{\sqrt{1 - \zeta_{c_k}^2}} ; \psi_{11_k} = \tan^{-1} \left(\frac{\sqrt{1 - \zeta_{c_k}^2}}{\zeta_{c_k}} \right) \quad (20)$$

4. Analytical Solution of EFW

The analytical solution for the structural behaviour of the EFW is developed in two parts that includes response to a pure flapping command as well as the EFW response to a flap angle command.

4.1 Periodic flapping response

Substituting $\ddot{w}_k(t)$ which gathered via Eq. (10), in Eqs. (3) and (7), yields the desired ordinary differential equation (ODE) for dynamic behaviour of the EFW under periodic actuation.

$$\ddot{\eta}_r(t) + 2\zeta_r \omega_r \dot{\eta}_r(t) + \omega_r^2 \eta_r(t) = \sum_{k=1}^3 \Gamma_k \left[e^{-\zeta_{c_k} \omega_{c_k} t} \sum_{j=1}^{\infty} \hat{A}_{22_{k,j}} \sin(\omega_{c_k} t + \hat{\phi}_{22_{k,j}}) + \sum_{j=1}^{\infty} \hat{A}_{11_{k,j}} \sin(\omega_{c_k} t + \hat{\phi}_{11_{k,j}}) \right] \quad (21)$$

where

$$\hat{A}_{22_{k,j}} = -A_{22_{k,j}} \omega_{c_k}^2 ; \hat{A}_{11_{k,j}} = -A_{11_{k,j}} \omega_{c_k}^2 ; \hat{\phi}_{22_{k,j}} = \phi_{22_{k,j}} + \tan^{-1} \left(\frac{2\zeta_{c_k} \sqrt{1 - \zeta_{c_k}^2}}{1 - 2\zeta_{c_k}^2} \right) ; \eta_r(0) = \eta_{r0} ; \dot{\eta}_r(0) = \dot{\eta}_{r0} \quad (22)$$

The analytical solution of this ODE is determined using the specified initial conditions.

$$\eta_r(t) = \sum_{k=1}^3 \sum_{j=1}^{\infty} \left[A_{1_{k,j}} \sin(\omega_{k,j} t + \phi_{1_{k,j}}) + e^{-\zeta_{c_k} \omega_{c_k} t} A_{2_{k,j}} \sin(\omega_{dc_k} t + \phi_{2_{k,j}}) \right] + e^{-\zeta_r \omega_r t} A_3 \sin(\omega_{dr} t + \phi_3) \quad (23)$$

where

$$\omega_{dr} = \omega_r \sqrt{1 - \zeta_r^2} \quad (24)$$

$$A_3 = \frac{\eta_{r0} - \sum_{k=1}^3 \sum_{j=1}^{\infty} [A_{1k,j} \sin(\phi_{1k,j}) + A_{2k,j} \sin(\phi_{2k,j})]}{\sin(\phi_3)} \quad (25)$$

$$\phi_3 = \tan^{-1} \frac{\sqrt{1 - \zeta_r^2} \tilde{\phi}_3}{\frac{\dot{\eta}_{r0}}{\omega_r} - \sum_{k=1}^3 \sum_{j=1}^{\infty} \left\{ A_{1k,j} \frac{\omega_{k,j}}{\omega_r} \cos(\phi_{1k,j}) + A_{2k,j} \frac{\omega_{c_k}}{\omega_r} \sin \left(\phi_{2k,j} - \tan^{-1} \frac{\sqrt{1 - \zeta_{c_k}^2}}{\zeta_{c_k}} \right) \right\} + \zeta_r \tilde{\phi}_3} \quad (26)$$

$$\tilde{\phi}_3 = \eta_{r0} - \sum_{k=1}^3 \sum_{j=1}^{\infty} [A_{1k,j} \sin(\phi_{1k,j}) + A_{2k,j} \sin(\phi_{2k,j})] \quad (27)$$

$$A_{2k,j} = - \frac{A_{22k,j} \Gamma_{\tilde{\kappa}}}{\sqrt{\left[\left(\frac{\omega_r}{\omega_{c_k}} \right)^2 - (1 - 2\zeta_{c_k}^2) - 2\zeta_r \zeta_{c_k} \left(\frac{\omega_r}{\omega_{c_k}} \right) \right]^2 + \left(2\zeta_r \sqrt{1 - \zeta_{c_k}^2} \left(\frac{\omega_r}{\omega_{c_k}} \right) - 2\zeta_{c_k} \sqrt{1 - \zeta_{c_k}^2} \right)^2}} \quad (28)$$

$$A_{1k,j} = \frac{-\Gamma_{\tilde{\kappa}} \left(\frac{\omega_{k,j}}{\omega_r} \right)^2 A_{11k,j}}{\sqrt{\left[1 - \left(\frac{\omega_{k,j}}{\omega_r} \right)^2 \right]^2 + \left[2\zeta_r \left(\frac{\omega_{k,j}}{\omega_r} \right) \right]^2}} \quad (29)$$

$$\phi_{2k,j} = \hat{\phi}_{22k,j} - \tan^{-1} \left(\frac{2\zeta_r \frac{\omega_r}{\omega_{c_k}} \sqrt{1 - \zeta_{c_k}^2} - 2\zeta_{c_k} \sqrt{1 - \zeta_{c_k}^2}}{\left(\frac{\omega_r}{\omega_{c_k}} \right)^2 - 2\zeta_r \zeta_{c_k} \frac{\omega_r}{\omega_{c_k}} - (1 - 2\zeta_{c_k}^2)} \right) \quad (30)$$

$$\phi_{1k,j} = \hat{\phi}_{11k,j} - \tan^{-1} \left(\frac{2\zeta_r \frac{\omega_{k,j}}{\omega_r}}{1 - \left(\frac{\omega_{k,j}}{\omega_r} \right)^2} \right) \quad (31)$$

The resulting analytical solution (Eqs. (23)-(31)) indicates that larger natural frequencies of the structural mode shapes tend to have no significant effect on the EFW dynamic behaviour. In addition, it is also seen that at structure-actuator frequency ratio (SAFR) close to one, i.e., $\omega_r/\omega_c \rightarrow 1$, existence of the actuation damping, ζ_c effectively bounds A_2 (Eq. (28)) that in turn prevents the second term of the EFW dynamic response (Eq. (23)) from growing. To check the conditions for other resonance behaviours, other coefficients will also be examined.

In this respect, when there is insignificant or zero structural damping, $\zeta_r \rightarrow 0$, A_1 and consequently A_3 tend towards infinity at structure-flapping frequency ratio (SFFR) close to one, i.e., $\omega_f/\omega_r \rightarrow 1$. Fig. 1 shows the variation of A_1 for two different values of ζ_r as a function of SAFR and SFFR. According to this figure, it is seen that A_1 achieves its pick value for resonance

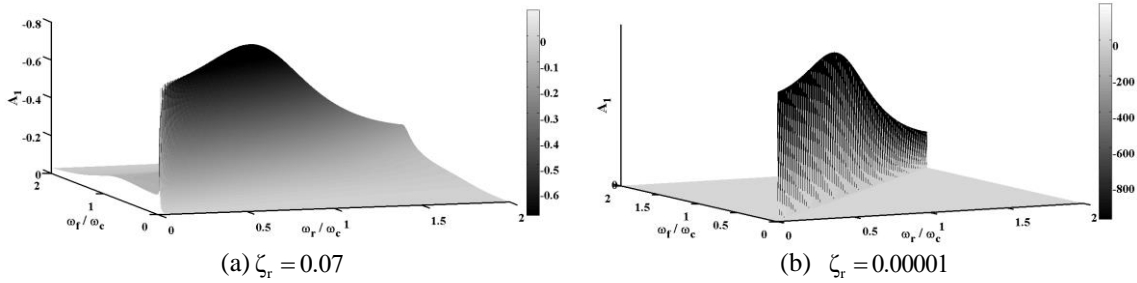


Fig. 1 The variation of A_1 values versus frequency ratios

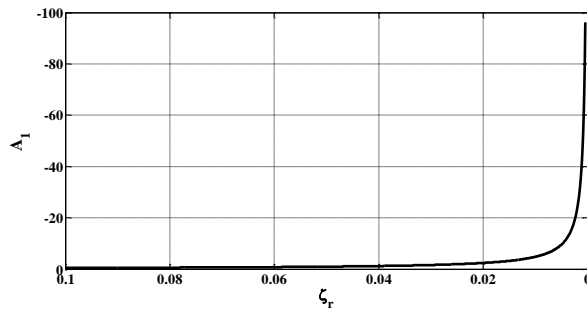


Fig. 2 The variation of A_1 values versus structural damping ratio at $\omega_r/\omega_c = \omega_f/\omega_c = 1$

conditions of both frequency ratios, i.e., $\omega_f/\omega_r \rightarrow 1$ and $\omega_r/\omega_c \rightarrow 1$. Finally, Fig. 2 shows the variation of A_1 at resonance conditions as a function of the EFW structural damping ζ_r .

4.2 Response to flap angle (glide) command

In analogy with the sinusoidal forcing the ODE governing EFW structural dynamic response is

$$\ddot{\eta}_r(t) + 2\zeta_r \omega_r \dot{\eta}_r(t) + \omega_r^2 \eta_r(t) = \sum_{k=1}^3 \Gamma_{\eta_k} \hat{B}_{11k} e^{-\zeta_{c_k} \omega_{c_k} t} \sin(\omega_{dc_k} t + \hat{\psi}_{11k}) \quad ; \quad \eta_r(0) = \eta_{r0} \quad ; \quad \dot{\eta}_r(0) = \dot{\eta}_{r0} \quad (32)$$

where

$$\hat{B}_{11k} = B_{11k} \omega_{c_k}^2 \quad ; \quad \hat{\psi}_{11k} = \psi_{11k} + \tan^{-1} \left(\frac{2\zeta_{c_k} \sqrt{1 - \zeta_{c_k}^2}}{1 - 2\zeta_{c_k}^2} \right) \quad (33)$$

Similarly, respective analytical solution is obtained as

$$\eta_r(t) = \sum_{k=1}^3 \left[e^{-\zeta_r \omega_r t} B_{2k} \sin(\omega_{dr} t + \psi_{2k}) + B_{1k} e^{-\zeta_{c_k} \omega_{c_k} t} \sin(\omega_{dc_k} t + \psi_{1k}) \right], \quad r = 1, 2, \dots \quad (34)$$

where

$$\psi_{2k} = \tan^{-1} \left\{ \frac{\frac{\omega_r}{\omega_{c_k}} \sqrt{1 - \zeta_r^2} (\eta_{r0} - B_{1k} \sin(\psi_{1k}))}{\frac{\dot{\eta}_{r0}}{\omega_{c_k}} - B_{1k} \sqrt{1 - \zeta_{c_k}^2} \cos(\psi_{1k}) + \zeta_{c_k} B_{1k} \sin(\psi_{1k}) + \zeta_r \frac{\omega_r}{\omega_{c_k}} (\eta_{r0} - B_{1k} \sin(\psi_{1k}))} \right\} \quad (35)$$

$$B_{2k} = \frac{\eta_{r0} - B_k \sin(\psi_{1k})}{\sin(\psi_{2k})} \tag{36}$$

$$B_k = \frac{\frac{\Gamma_{r_k} \Delta \bar{\sigma}_{\text{glide}_k}}{\sqrt{1 - \zeta_{c_k}^2}}}{\sqrt{\left[2 \left(\frac{\omega_r}{\omega_{c_k}} \right) \zeta_r \sqrt{1 - \zeta_{c_k}^2} - 2 \zeta_{c_k} \sqrt{1 - \zeta_{c_k}^2} \right]^2 + \left[\left(\frac{\omega_r}{\omega_{c_k}} \right)^2 - (1 - 2 \zeta_{c_k}^2) - 2 \left(\frac{\omega_r}{\omega_{c_k}} \right) \zeta_r \zeta_{c_k} \right]^2}} \tag{37}$$

$$\psi_{1k} = \hat{\psi}_{11k} - \tan^{-1} \left(\frac{2 \left(\frac{\omega_r}{\omega_{c_k}} \right) \zeta_r \sqrt{1 - \zeta_{c_k}^2} - 2 \zeta_{c_k} \sqrt{1 - \zeta_{c_k}^2}}{\left(\frac{\omega_r}{\omega_{c_k}} \right)^2 - (1 - 2 \zeta_{c_k}^2) - 2 \left(\frac{\omega_r}{\omega_{c_k}} \right) \zeta_r \zeta_{c_k}} \right) \tag{38}$$

5. Case study

To better understand the EFW dynamic behaviour subsequent to commanded flapping, a case study is performed where the commanded flapping is a sinusoidal motion whose analytical solution have already been developed. It needs to be mentioned that the EFW natural frequencies and mode shapes are required for dynamic response analysis and calculated via FEM. To analyse the EFW structural response, a flapping scenario is considered where the actuator initially commands a sinusoidal behaviour (from rest).

5.1 Simulation considerations

In this study, only the right wing is modelled and simulated, while the EFW body is considered

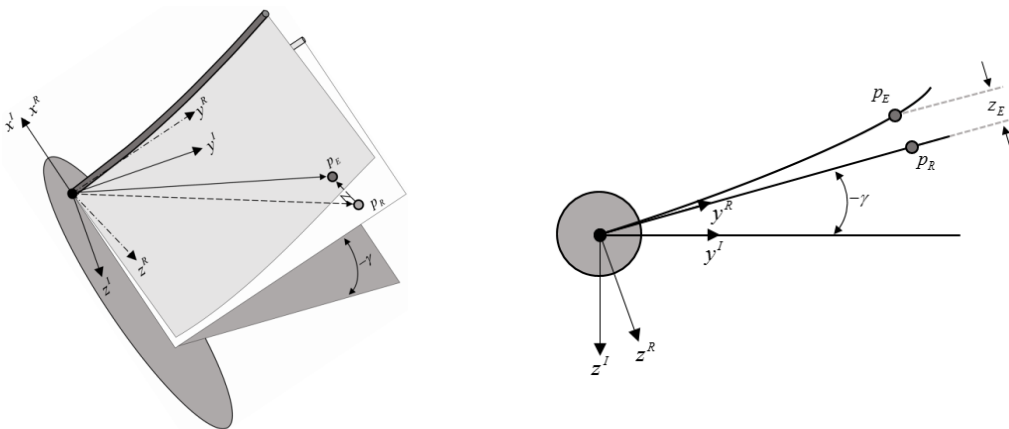


Fig. 3 Flapping wing Coordinates systems Definition

motionless and fixed to an inertial coordinate system (ICS). Therefore, one can specify the EFW rigid motion via a single flapping angle with respect to the ICS. Accordingly, EFW elements will experience a vibrating motion in addition to the aforementioned prescribed rigid body motion as shown in Fig. 3. As a result, the total inertial position of EFW elements can be computed via superposition of its rotational position plus an elastic deformation emanating from the EFW analytical solutions presented.

Additionally, the origin of the ICS is taken at the EFW hinge located at the wing root leading edge point, where x^I points forward, z^I points downward within the EFW plane of symmetry and y^I axis is perpendicular to the previous directions to form a right handed orthogonal system (see Fig. 3). Moreover, a rigid body coordinate system is defined that shows the EFW elements rigid motion via the flapping angle γ . The subscript I , R and E are indicative of ICS, rigid EFW local body coordinate system and the elastic local deformation of a typical point on R, respectively. Finally, one can obtain the coordinates of any arbitrary point, P_E with respect to the ICS as, (see Fig. 4).

$$\begin{bmatrix} x^I \\ y^I \\ z^I \end{bmatrix} = \begin{bmatrix} 1 & 0 & 0 \\ 0 & \cos(-\gamma) & \sin(-\gamma) \\ 0 & -\sin(-\gamma) & \cos(-\gamma) \end{bmatrix} \begin{bmatrix} x^R \\ y^R \\ z^E \end{bmatrix} = \begin{bmatrix} x^R \\ y^R \cos(\gamma) - z^E \sin(\gamma) \\ y^R \sin(\gamma) + z^E \cos(\gamma) \end{bmatrix} \quad ; \quad z^E = \sum_r \eta_r(t) \phi_r(P) \quad (39)$$

5.2 Structural considerations

The rectangular wing considered in this study (Fig. 3) is modelled as cantilever structure. This is because the wing structure is practically being carried by the servomotor connector bar where the EFW is fixed to this connector bar at the junction.

Despite the fact that the extracted relations in section III are independent of the structural elements type for FEM analysis, the EFW structure is considered as a reinforced rectangular structure (RRS). The RRS is modelled as a flat plate with dimensions of $1(mm) \times 300(mm) \times 500(mm)$, reinforced at the leading edge (LE) by a tubular beam of radius 2 mm that adds to the flexural strength about the x^R axis. Further, the RRS Aluminium wing has stiffness properties $E=70\text{ Gpa}$, $G=26\text{ Gpa}$ and a mass density of $\rho=2710\text{ kg/m}^3$ (Beer *et al.* 2011).

The modal properties of the EFW are determined via FEM which consists of 25×15 beam and shell elements, where the first 5 modes are taken into account, see Table 1. The EFW is modelled via elements

Table 1 Modal structural properties of first 10 modes

Mode Number	Natural frequency (Hz)	Generalized Inertial Moment (kg.m)
1	2.56	0.1837
2	6.81	-0.0334
3	16.57	-0.0178
4	27.11	0.0092
5	44.33	0.0064

In order to verify the analytical structural solution of the EFW, the commercial Nastran-Patran (MSC Nastran 2010) (NASP) FEM code is utilized whose transient response results for a time-

dependent point force, $(f(t)=0.1\sin(2\pi t))$ where $0 < t < 1$ applied to the arbitrary point, C , located at the trailing edge of tip section, is shown in Fig. 5. This figure compares the analytically calculated elastic displacement of C against the transient response result of NASP as well as Newmark time-integration method. As demonstrated in this figure, all three results coincide and thus the proposed analytical solution is accurate and compatible with no-planner-displacement assumption.

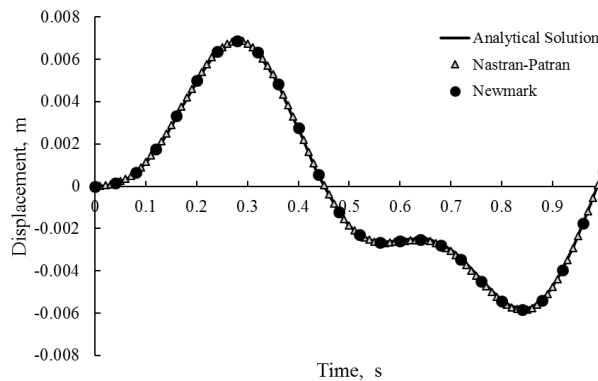


Fig. 5 Elastic displacement of point C, from analytical solution versus the transient response in NASP

5.3 Simulation and results

The EFW simulation parameters are listed in Table 2. According to the aforementioned flight scenarios, simulations of the EFW flapping and gliding motion are performed continuously and consecutively.

Table 2 EFW simulation parameters

Parameters (Input)	Value	Parameters (Calculated)	Value
t_{Glide} (sec)	4.2	A_{21}	0.4958
ω_f (rad/sec)	2π	A_{22}	0.6020
γ_{max} (deg)	30	ϕ_{22}	0.9675
γ_{Glide} (deg)	5	A_{11}	0.4979
ζ_c	0.5	ϕ_{11}	-1.6628
ω_c (rad/sec)	6	B_{11}	0.1008
ζ_r	0.07	ψ_{11}	1.0472

It needs to be mentioned that the number of required modes is problem dependent and it is found that three modes are sufficient with an accuracy of 0.1%. Finally, the EFW motion is animated under the influence of the controller dynamics in Fig. 6 at different time steps.

Additionally, in a more accurate analysis, the simulation was run for various SFFR whose results for the maximum deformation is shown in Fig. 7. As seen, in general, for SFFR lower than

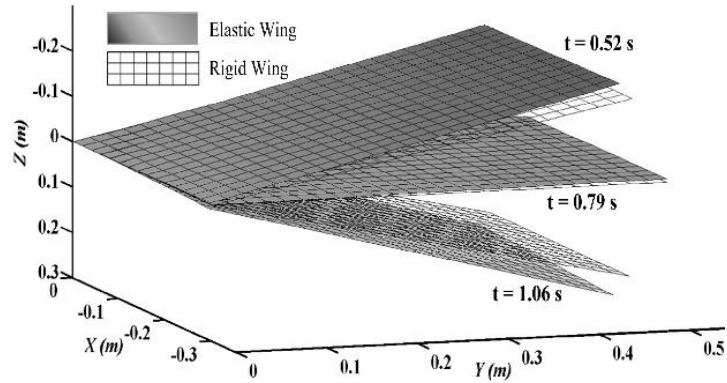


Fig. 6 Wing status at 1st cycle in 3 various step times

one, as SFFR increases, the maximum deformation also grows. But, considering the fact that in current case, actuator frequency is lower than first structural frequency, the mentioned trend has different behaviour around $\omega_f = \omega_c$.

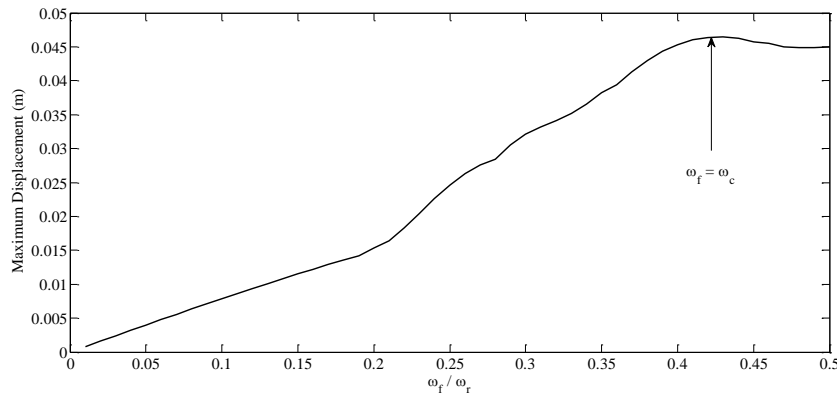


Fig. 7 maximum wing deformation for various SFFR

6. Conclusions

An analytical solution for the structural dynamics of an Elastic Flapping Wing (EFW) in Transient phase of flapping and gliding is presented using a reduced order model that is verified under a time-varying loading scenario. Due to importance of having an analytical solution for the EFW structural behaviour in order to conceptually analyse the effect of wing elasticity, the linear motion range assumption is stipulated. A common flight scenario of birds is simulated in which a wing starts a sinusoidal motion that is subsequently commended to stop at a fixed angular position while the servo dynamics is accounted for. In the undamped systems, it is realized that resonance occurs if structure-flapping frequency ratio (SFFR) equals to unity. On the other hand, the resonance won't occur in the damped system, but the maximum amplitude happens when both frequency ratios, structure-actuator frequency ratio (SAFR) and SFFR equal to unity. Analytical

investigations reveal that one does not need to consider all structural modes as the amplitude pertinent to generalized coordinates of the high-frequency modes tend towards zero. Although, due to importance and also simplicity, only the inertial force is considered in the EFW analysis, because of periodic nature of the aerodynamic and gravitational forces, they can be taken into account using periodic series such as Fourier in more comprehensive studies. In addition to the substantial analytical results, this study opens up a new perspective in flapping wing analysis that enables one to reach a better understanding of EFWs SD behaviour. The universal outcome of this study is that the expensive numerical approach can be intelligently substituted by mathematics-based one in EFW analysis.

Acknowledgments

The authors would like to thank Professor H. Haddadpour of Sharif University of Technology for his helpful suggestions in this study.

References

- Barut, A., Das, M. and Madenci, E. (2006). "Nonlinear deformations of flapping wings on a micro air vehicle", *Proceedings of the 47th AIAA/ASME/ASCE/AHS/ASC Structures, Structural Dynamics, and Materials Conference*, Newport, Rhode Island, U.S.A., May.
- Beer, F.P., Johnston, E.R., DeWolf, J.T. and Mazurek, D.F. (2011), *Mechanics of Materials*, McGraw-Hill, New York, U.S.A.
- Combes, S.A. and Daniel, T.L. (2003), "Into thin air: Contributions of aerodynamic and inertial-elastic forces to wing bending in the hawkmoth *manduca sexta*", *J. Exper. Biol.*, **206**(17), 2999-3006.
- Daniel, T.L. and Combes, S.A. (2002), "Flexible wings and fins: Bending by inertial or fluid-dynamic forces?", *Integr. Comparat. Biol.*, **42**(5), 1044-1049.
- De Rosi, A., Falcucci, G., Ubertini, S. and Ubertini, F. (2014), "Aeroelastic study of flexible flapping wings by a coupled lattice boltzmann-finite element approach with immersed boundary method", *J. Flu. Struct.*, **49**, 516-533.
- Heathcote, S., Wang, Z. and Gursul, I. (2008), "Effect of spanwise flexibility on flapping wing propulsion", *J. Flu. Struct.*, **24**(2), 183-199.
- Hollkamp, J.J. and Gordon, R.W. (2008), "Reduced-order models for nonlinear response prediction: Implicit condensation and expansion", *J. Sound Vibr.*, **318**(4), 1139-1153.
- Isogai, K. and Harino, Y. (2007), "Optimum aeroelastic design of a flapping wing", *J. Aircr.*, **44**(6), 2040-2048.
- Kim, D.K. and Han, H. (2008). "A dynamic model of a flexible flapping wing for fluid-structure interaction analysis", *Proceedings of the 15th International Congress on Sound and Vibration*, Daejeon, Korea, July.
- Larijani, R.F. and DeLaurier, J.D. (2001), "A nonlinear aeroelastic model for the study of flapping wing flight", *Progr. Astronaut. Aeronaut.*, **195**, 399-428.
- Li, Y., Nahon, M. and Sharf, I. (2009), "Dynamics modeling and simulation of flexible airships", *AIAA J.*, **47**(3), 592-605.
- Mazaheri, K. and Ebrahimi, A. (2010), "Experimental study on interaction of aerodynamics with flexible wings of flapping vehicles in hovering and cruise flight", *Arch. Appl. Mech.*, **80**(11), 1255-1269.
- McEwan, M., Wright, J., Cooper, J. and Leung, A. (2001). "A finite element/modal technique for nonlinear plate and stiffened panel response prediction", *Proceedings of the 42nd AIAA/ASME/ASCE/AHS/ASC Structures, Structural Dynamics, and Materials Conference and Exhibit Technical Papers*, Anaheim, California, U.S.A., June.

- Meirovitch, L. and Tuzcu, I. (2003), *Integrated Approach to the Dynamics and Control of Maneuvering Flexible Aircraft*, NASA/CR-2003-211748, National Aeronautics and Space Administration, Langley Research Center.
- MSC Nastran (2010), *MSC Nastran 2010 User's Manual*, MSC Software Corporation, Santa Ana, U.S.A.
- Nakata, T. and Liu, H. (2012), "A fluid-structure interaction model of insect flight with flexible wings", *J. Comput. Phys.*, **231**(4), 1822-1847.
- Ogata, K. (2010), *Modern Control Engineering*, Prentice Hall, Upper Saddle River, New Jersey, U.S.A.
- Olivier, M. and Dumas, G. (2016), "Effects of mass and chordwise flexibility on 2D self-propelled flapping wings", *J. Flu. Struct.*, **64**, 46-66.
- Platus, D. (1992), "Aeroelastic stability of slender, spinning missiles", *J. Guid. Contr. Dyn.*, **15**(1), 144-151.
- Pourtakdoust, S. and Assadian, N. (2004), "Investigation of thrust effect on the vibrational characteristics of flexible guided missiles", *J. Sound Vibr.*, **272**(1), 287-299.
- Pourtakdoust, S.H. and Aliabadi, S.K. (2012), "Evaluation of flapping wing propulsion based on a new experimentally validated aeroelastic model", *Sci. Iran.*, **19**(3), 472-482.
- Rizzi, S.A. and Muravyov, A.A. (2002), *Equivalent Linearization Analysis of Geometrically Nonlinear Random Vibrations Using Commercial Finite Element Codes*, NASA/TP-2002-211761, National Aeronautics and Space Administration.
- Shyy, W., Berg, M. and Ljungqvist, D. (1999), "Flapping and flexible wings for biological and micro air vehicles", *Progr. Aerosp. Sci.*, **35**(5), 455-505.
- Singh, B. and Chopra, I. (2007). "An aeroelastic analysis for the design of insect-based flapping wings", *Proceedings of the 48th AIAA/ASME/ASCE/AHS/ASC Structures, Structural Dynamics, and Materials Conference*, Honolulu, Hawaii, U.S.A., April.
- Smith, M. (1995), "The effects of flexibility on the aerodynamics of moth wings-towards the development of flapping-wing technology", *Proceedings of the 33rd Aerospace Sciences Meeting and Exhibit*, Reno, NV, U.S.A., January.
- Wilson, N. and Wereley, N. (2007), "Experimental investigation of flapping wing performance in hover", *48th AIAA/ASME/ASCE/AHS/ASC Structures, Structural Dynamics, and Materials Conference*, Honolulu, Hawaii, U.S.A., April.
- Wootton, R.J. (1992), "Functional morphology of insect wings", *Ann. Rev. Entomol.*, **37**(1), 113-140.
- Yeo, D., Atkins, E.M., Bernal, L.P. and Shyy, W. (2013), "Experimental characterization of lift on a rigid flapping wing", *J. Aircr.*, **50**(6), 1806-1821.
- Zhao, L., Huang, Q., Deng, X. and Sane, S.P. (2010), "Aerodynamic effects of flexibility in flapping wings", *J. Roy. Soc. Interf.*, **7**(44), 485-497.